Unpicking vibration-vibration and vibration-torsion interactions in *m*-fluorotoluene

Alexander R. Davies, David J. Kemp, and Timothy G. Wright[a]

School of Chemistry, University of Nottingham, University Park, Nottingham NG7 2RD, UK

[a] Tim.Wright@nottingham.ac.uk

ABSTRACT

Two-dimensional laser-induced fluorescence (2D-LIF) spectra are reported for a set of features in the $S_1 \leftrightarrow S_0$ electronic spectrum of *m*-fluorotoluene. Two transitions previously assigned to fundamentals are reassigned in the present work. The main reassignments are confirmed with zero-electron-kinetic-energy (ZEKE) spectroscopy. Interactions in the S_0, S_1 and D_0^+ electronic states involving vibrational and vibration-torsional ("vibtor") levels are identified via observed activity. The obtained vibrational wavenumbers compare well to the results of quantum chemical calculations.

Keywords

m-fluorotoluene, REMPI, ZEKE, dispersed fluorescence, 2D-LIF, LIF, torsion, vibration, fluorescence, ionization.

[a] Timothy G. Wright,
Professor of Physical and Theoretical Chemistry,
School of Chemistry,
University of Nottingham,
University Park,
Nottingham NG7 2RD
Phone: +44 115 8467076
FAX: +44 115 9513562
Email: Tim.Wright@nottingham.ac.uk

1. Introduction

In previous work[1,2,3] we have presented assignments of bands seen in the $S_1 \leftrightarrow S_0$ electronic spectra of *m*-fluorotoluene (*m*FT), based on activity seen in resonance-enhanced multiphoton ionization (REMPI), two-dimensional-LIF (2D-LIF) and zero-electron-kinetic-energy (ZEKE) spectra, together with quantum chemical calculations. The first work[1] focused on the low-energy region, the second[2] on unusual intensities caused by Duschinsky rotations, with the most recent one[3] tackling the majority of the bands in the 0–1350 cm^{-1} region of the $S_1 \leftarrow S_0$ transition. In the latter paper, we examined the evolution of the interactions that underpin intramolecular vibrational energy redistribution (IVR) from the restricted regime through to that of statistical; furthermore, the validity of directly comparing the IVR behaviour of *m*- and *p*-fluorotoluene was considered. Omitted from Ref. 3 was a detailed consideration of the bands in the 650–800 cm^{-1} region, shown in Figure 1, except for the assignment of the $17^1m^{0,1}$ contributions. In the present work, we consider this region of the spectrum further. We present both 2D-LIF and ZEKE spectra, and discuss evidence for the assignment of the main contributions to these features, together with evidence for interactions in the S_0, S_1 and D_0^+ states.

Our first paper on the low-wavenumber region[1] complemented the 2D-LIF study of that region by Stewart, Gascooke and Lawrance,[4] and information from both papers is useful in aiding the assignment of the spectra reported in the present work. Also in Ref. 4, quantum chemistry calculations suggested that several of the assignments by Okuyama et al.[5] may be incorrect, and this was supported by similar calculations by ourselves.[3] The present work will consider two of these, providing spectroscopic evidence for the reassignments. The activity will then be seen to be consistent with that seen in the corresponding region for *m*-difluorobenzene (*m*DFB)[6] – see Figure 1.

2. Experimental

The REMPI/ZEKE[7] and 2D-LIF[8] apparatuses are the same as those employed recently. In all of the present experiments, a free-jet expansion of the vapour above room-temperature *m*FT (Sigma-Aldrich, 98% purity) in 2 bar Ar was employed.

For the 2D-LIF spectra, the free-jet expansion was intersected at *X*/*D* ~20 by the frequency-doubled output of a single dye laser (Sirah CobraStretch), operating with Coumarin 503 and pumped with the third harmonic of a Surelite III Nd:YAG laser. The fluorescence was collected, collimated, and focused onto the entrance slits of a 1.5 m Czerny-Turner spectrometer (Sciencetech 9150) operating in single-pass mode, dispersed by a 3600 groove/mm grating. This allowed ~300 cm^{-1} windows of the dispersed fluorescence to be collected by a CCD camera (Andor iStar DH334T). At a fixed grating angle of the spectrometer, the excitation laser was scanned, and at each excitation wavenumber the camera image was accumulated for 2000 laser shots. This allowed a plot to be produced of fluorescence intensity versus both the excitation laser wavenumber and the wavenumber of the emitted and dispersed fluorescence, termed a 2D-LIF spectrum.[9,10]

The REMPI and ZEKE spectroscopic experiments employed focused, frequency-doubled dye laser outputs (Sirah CobraStretch). For the ZEKE experiments, two such outputs were overlapped spatially and temporally, and passed through a vacuum chamber coaxially and counterpropagating, where they intersected the free-jet expansion. The excitation laser (also used in the REMPI experiments) operated with Coumarin 503 and was pumped with the third harmonic (355 nm) of a Surelite III Nd:YAG laser, while the ionization laser operated with Pyrromethene 597, pumped with the second harmonic (532 nm) of a Surelite I Nd:YAG laser. The jet expansion passed between two biased electrical grids located in the extraction region of a time-of-flight mass spectrometer, which was employed in the REMPI experiments. These grids were also used in the ZEKE experiments by application of pulsed voltages, giving typical fields of ~10 V cm^{-1}, after a delay of up to 2 μs; this delay was minimized while avoiding the introduction of excess noise from the prompt electron signal. The resulting ZEKE bands had widths of ~5–7 cm^{-1}. Electron and ion signals were recorded on separate sets of microchannel plates.

3. Nomenclature

3.1. Vibrational and Torsional Labelling

When referring to vibrations, the C_s point group may be used, under the assumption that the methyl group may be treated as a point mass. To consider the methyl torsional motion explicitly, use of the G_6 molecular symmetry group (MSG) is appropriate. In Table 1, we provide the correspondence between the C_s and G_6 symmetry labels. The torsional levels will be labelled via their m quantum number.[1,4] We shall employ the D_i labels[11] for the vibrations, as used in previous work.[1,2,3,4] That labelling scheme is based on the vibrations of the *m*DFB molecule, but treated within the C_s point group. The available experimental vibrational wavenumbers for *m*FT and *m*DFB are presented in Table 2, alongside the calculated wavenumbers – the majority of the calculated values have been presented previously.[3] Diagrams of the atomic motions associated with each D_i label can be found in Ref. 11. One caveat to this is that the D_{19} and D_{20} the motions are very mixed in the S_1 state (only) of *m*FT, as discussed in Ref. 2, and are denoted therein as D_X and D_Y respectively in that state; we retain that labelling here.

To establish the overall symmetry of a vibtor level, it is necessary to use the corresponding G_6 label for the vibration, and then find the direct product with the symmetry of the torsion, noting that a C_{3v} point group direct product table can be used, since the G_6 MSG and the C_{3v} point group are isomorphic.

Under the free-jet expansion conditions employed here, almost all molecules are expected to be cooled to their zero-point vibrational level, and thus essentially all $S_1 \leftarrow S_0$ pure vibrational excitations are expected to originate from this level. In contrast, owing to nuclear-spin and rotational symmetry, the molecules can be in one of the $m = 0$ or $m = 1$ torsional levels,[12] with close-to-equal populations in each; additionally, residual population in the $m = 2$ level of *m*FT is sometimes present.[1,4,5]

3.2. Coupling and transitions

In the usual way, vibrational transitions will be indicated by the number, i, of the D_i vibration, followed by a super-/subscript specifying the number of quanta in the upper/lower states, respectively; torsional transitions will be indicated by m followed by its value. Finally, vibtor transitions will be indicated by a combination of the vibrational and torsional transition labels. When designating transitions, we shall generally omit the initial level, since it will be obvious from either the jet-cooled conditions or the specified intermediate level. When we refer to a "vibrational transition" it is understood to refer to both the $m = 0$ and $m = 1$ components, unless otherwise specified.

As has become common usage, we will generally refer to a level by specifying quantum numbers, thus: superscripts indicate levels in the S_1 state; and subscripts indicate levels in the S_0 state; since we will also be referring to transitions and levels involving the ground state cation, D_0^+, we shall indicate those as superscripts, but with a single, additional, preceding superscripted "+" sign. Relative wavenumbers of the levels will be given with respect to the relevant zero-point vibrational and m level in each electronic state.

For cases where the geometry and the torsional potential are both similar in the S_1 and D_0^+ states, the most intense transition is usually expected to be that for which no changes in the torsional and/or vibrational quantum numbers occur, designated as $\Delta m = 0$, $\Delta v = 0$, or $\Delta(v, m) = (0, 0)$ transitions, as appropriate. Where we are denoting the difference in quantum numbers between a pair of interacting levels as $\Delta(v, m) = (x, y)$, where x denotes the change in the vibrational quantum number, and y that in the torsional quantum number.

However, as will be seen (and as reported in Refs. 1, 4 and 5), the $\Delta m = 0$ and $\Delta(v, m) = (0, 0)$ transitions are almost always not the most intense bands in the ZEKE spectra for *m*FT, indicative of a significant change in the torsional potential upon ionization. The assignments and intensities of low-wavenumber features in the $S_1 \leftrightarrow S_0$ transitions have been discussed in Ref. 4, and reference will be made to that work when appropriate; the corresponding ZEKE spectra have been considered in depth in Ref. 1.

When we need to refer to the wavenumbers of a 2D-LIF band, this will be done as a (excitation, emission) cm^{-1} pair of numbers; similarly, a pair of transitions can be explicitly given[4] if required to identify a 2D-LIF band.

If two levels are close in wavenumber, and have the same overall symmetry, then (except between vibrational fundamentals, to first order) interactions can occur. The simplest example of this is the anharmonic interaction between two vibrational levels – the classic Fermi resonance,[13] where the intensity of an optically bright state – a zero-order bright (ZOB) state – may be thought of as being shared with an optically dark state – i.e. zero-order dark (ZOD) state; ZOB and ZOD states can be referred to collectively as zero-order states (ZOSs). Further couplings can also occur, and multiple couplings can be considered within the "tier model",[14] with the overall process being termed intramolecular vibrational redistribution (IVR). Direct couplings are only expected to be significant for small changes, $\Delta v \approx 3$, of the vibrational quantum number.[15] For molecules that contain a hindered internal rotor, and if vibration-torsion coupling occurs, then interactions can also involve torsional and/or "vibtor" levels. This is expected to be significant only for changes in the torsional quantum number Δm, of 0, ±3 or ±6, in descending order of likely strength.[16] The end result of such interactions is the formation of eigenstates with mixed character. Often the resulting eigenstates will be referred to herein by the dominant contribution, with the context implying if an admixture is present. If this process involves only a handful of states, this is known as restrictive IVR whereas, if there is widespread dispersal of internal energy, this is known as statistical IVR.

4. Assignments

The assignments of the majority of the bands in the ~0–1350 cm^{-1} region of the electronic spectrum of the $S_1 \leftarrow S_0$ transition in *m*FT have been discussed in our previous work.[1,2,3] Here we focus on the 650–800 cm^{-1} region, for which the REMPI spectrum is shown in Figure 1, together with the corresponding section of the *m*DFB spectrum. (Scans of the wider ~0–1350 cm^{-1} regions have been presented in Ref. 3, where the activities were compared between these two molecules.)

We shall consider each main feature of the *m*FT spectrum by discussing the 2D-LIF spectra, considering pertinent bands and regions, before moving onto the ZEKE spectra. The latter turn out to be less useful in the initial identification of the assignments of the various contributions to the spectra, owing to the change in phase and other torsional parameters between the S_1 state and the cation. This aspect leads to several ZEKE bands arising for each contribution, and while this is a useful diagnostic in cases where there is a highly dominant contribution,[1,2,3] it leads to complicated spectra; even so, the ZEKE spectra provide useful confirmatory evidence for the main assignments.

We have recorded 2D-LIF spectra of *m*FT across the excitation range 676–748 cm^{-1}, and in the emission range 25–1300 cm^{-1}; this latter range is expected to cover the $\Delta(v, m)$ = (0, 0) regions, as well as showing other activity indicative of interactions with vibtor levels. In Figure 2, we show two sections of the overview of the 2D-LIF spectrum where the richness of the emission activity can be seen. The larger region covers the $\Delta(v, m)$ = (0, 0) regions, while the smaller section shows the low-wavenumber emission region when exciting across the same region of bands. At the top of Figure 2 we show the result of vertically integrating the 2D-LIF spectrum, producing a spectrum that is very similar to the corresponding region of the REMPI spectrum shown in Figure 1; this suggests that the range of the fluorescence collected in the 2D-LIF image is representative of the absorption spectrum. It is relatively straightforward to see columns of emission activity in the 2D-LIF spectrum, and to associate these with the individual excitation features; however, it can be seen that there is extra complexity underlying each feature.

The change in the torsional potential between the S$_0$ and S$_1$ states leads to the origin, and other vibrational bands in the REMPI and integrated fluorescence spectrum (see Figure 1), to comprise a pair of bands corresponding to Δm = 0 transitions involving the m = 0 and m = 1 components, of roughly equal intensity, and separated by ~ 4 cm^{-1}.[1,4,5] As such, it is expected that there will be columns of emission bands in the 2D-LIF spectrum, arising from pairs of approximately equal intensity transitions. Additionally, there are various vibtor transitions, some of which are those accessible from each of the S$_1$ m = 0, 1 components.[1,2,3,4,5] Interestingly, for the 675–690 cm^{-1} and 734–746 cm^{-1} excitations, there is not a single pair of obvious $\Delta(v, m)$ = (0, 0) bands corresponding to each ZOB state. Furthermore, across the 2D-LIF spectrum, in the cases where they are present, the intensities of the m = 0 and m = 1 components of various 2D-LIF bands may be seen to be markedly different to one another (Figure 2). Not so obvious, is that there are various emission bands that are not directly associated with an active vibrational level, and so must arise as a result of interactions; for the most part, these are assigned to vibtor levels.

In previous work,[3] we have discussed the 2D-LIF and ZEKE spectra recorded across the 675–690 cm^{-1} absorption region. The ZEKE spectra were clear that the main contribution to this region was $17^1m^{0,1}$, with the distinctive pattern of associated $^{+}17^1m^x$ vibtor bands. Interestingly, as may be seen from Figure 2, as well as the clear $17_1m_{0,1}$ emission bands in the 2D-LIF spectrum, there are other fairly strong emission bands to higher wavenumber, in particular $15_1m_{0,1}$, even though the calculated Duschinsky mixing of the D_{15} and D_{17} vibrations was minimal – indeed, when exciting $15^1m^{0,1}$, the

$17_1m_{0,1}$ bands were actually more intense than the $15_1m_{0,1}$ ones.[3] Although these transitions are allowed, it is possible that the vibrational potentials are affected by vibronic coupling, which was not included in the calculation of the Duschinsky matrix.

If we use the same labelling scheme for *m*DFB and *m*FT, then, since the masses of the substituents are very similar, we expect the corresponding vibrational wavenumbers to be close for these molecules, although some differences may arise from electronic/steric factors.[11] As a consequence, in assigning the REMPI spectrum of *m*FT, we expect activity to resemble that seen in corresponding spectra of other similar molecules, such as the LIF and REMPI spectra of *m*DFB.[3,6] In Figure 1, we have included the corresponding section of the REMPI spectrum of *m*DFB, which is similar in appearance to that of the LIF spectrum of Ref. 6, where assignments of a number of bands are given, and with which we largely concurred;[3] the additional *m*FT assignments will be discussed in the following subsections.

Stewart et al.[4] reported scaled harmonic wavenumbers for the vibrations of *m*FT obtained with quantum chemistry calculations, and we reported very similar calculated values.[1,2,3] These calculations indicated that the two main higher-wavenumber, 698–714 cm^{-1} and 734–746 cm^{-1}, excitation features are not assignable to the fundamentals suggested by Okuyama et al.[5] We will reassign these bands herein, based on the activity seen in the 2D-LIF and ZEKE spectra, and consistent with the quantum chemical calculations.

4.1 The 17^1 level

Concentrating first on the activity in the absorption range 675–690 cm^{-1} – see expanded view of the 2D-LIF image in Figure 3 – the strongest emission may be seen to be at a wavenumber of 731 cm^{-1}, which has been assigned[3,5] to 17_1. However, the intensity of the 17_1m_0 band is significantly stronger than that of 17_1m_1, suggesting that the 17^1m^1 level is interacting with other S_1 levels and/or is emitting to more levels than 17^1m^0. Clearly, the overall intensity profile of the REMPI/LIF feature suggests that the integrated emissions for the two *m* components are relatively similar (see traces at the top of Figure 2 and Figure 3), although the $17^1m^{0,1}$ band profiles are significantly different to those of the $m^{0,1}$ band associated with the adiabatic transition (see insert in Figure 1), suggestive of an interaction occurring for one or both of the $17^1m^{0,1}$ levels. In Figure 3, we have given assignments of many of the more-intense bands – it is clear that there are many other weaker bands in the spectrum, but we refrain from discussing all of these, concentrating on establishing the main assignments and hence interactions.

Since D_{17} is a totally-symmetric vibration, then it is not surprising that the most intense emission bands correspond to Franck-Condon (FC)-active totally-symmetry vibrations, many of which were also seen when exciting the origin;[3] indeed, the 17_1 emission was the strongest emission observed when exciting via the origin.[3] Each vibrational band in the REMPI and 2D-LIF spectra has the expected "double band" structure, arising from m^0 and m^1 component transitions, and also associated vibtor levels, similar to those seen on the origin;[1,4] and although some are too weak to discern in Figure 3, many can be seen on "zoomed-in" views (not shown). In Figure 2, the low-wavenumber emission region of the 2D-LIF spectrum is presented, and we highlight the clear $m_{3(+)}$ band when exciting 17^1m^0, and the m_4 band seen when exciting 17^1m^1 (the expected m_2 band was obscured by scatter from the excitation laser, and is not present in Figure 2).

It is evident from Figure 3, that the bands corresponding to totally-symmetry vibrations all have a m_0 component that is more intense than the m_1 one. Examination of other activity reveals that there are a number of 2D-LIF bands that are not associated with FC activity, primarily corresponding to S_1 levels of e symmetry, and so arising directly from, or potentially via interaction with, 17^1m^1. Furthermore, several of the bands have activity extending to higher excitation wavenumber than 17_1m_0, notably the emission band at 1079 cm^{-1}.

Since the wavenumbers of the majority of the S_0 fundamentals have been established,[1,2,3,4,5] and since the torsional spacings are also known, then the majority of the emission bands can be assigned with a fair degree of confidence, noting that anharmonicity together with vibrational and vibration-torsion interactions may lead to bands being slightly displaced from the expected positions.[4]

We now move on to consider other bands in the 2D-LIF spectrum, that do not appear to be associated with emissions arising from the FC-active totally-symmetric vibrations and their vibtors. These "additional" bands can arise as a result of interactions, in which case we should be able to identify them from a combination of their excitation and emission wavenumbers, or as activity associated with the main excitations. We first address the feature that appears as a shoulder on high-wavenumber side of the 17^1m^0 band (see trace at top of Figure 3), which is consistent with emission producing the high-wavenumber contribution to the band at (687, 1079) cm^{-1}. (We associate the majority of the lower-excitation portion of the 1079 cm^{-1} emission feature with FC-activity arising from 14_1 following excitation of 17^1, as seen via the origin, and assigned in Ref. 3.)

As the (687, 1079) cm^{-1} feature corresponds to the most intense emission at this excitation wavenumber, we conclude this 2D-LIF feature is a $\Delta(v, m) = (0, 0)$ band, and so corresponds to a level that involves one or more vibrations that have a significant shift between the S_0 and S_1 states. Consideration of the possibilities reveals two contenders: ($24^130^1m^2$, $24_130_1m_2$) and ($24^129^1m^{0,1}$, $24_129_1m_{0,1}$). Considering initially the $24^130^1m^2$ level, this can interact with 17^1m^1, consistent with the lower intensity of the 17^1m^1 transition, and associated transitions; this would be a $\Delta(v, m) = (3, 3)$ interaction. This would then imply that the FC-active emission bands that occur at an excitation wavenumber of 681 cm^{-1} arise from $17^1m^1\ldots24^130^1m^2$, while those that occur at an excitation wavenumber of 687 cm^{-1} arise from $24^130^1m^2\ldots17^1m^1$, where the first term indicates the dominant contribution to that eigenstate; other contributions to these eigenstates would also likely be occurring. However, the band profiles of other emission bands at this excitation wavenumber are more in line with a totally-symmetric level, and particularly that there is an additional overlapping contribution to the m_0 components, and an extended activity to higher excitation wavenumber (most clearly seen on the 1079 cm^{-1} emission). The most convincing evidence for assigning this emission to a totally-symmetric level is that this extends to higher emission wavenumber for $17_1m_{3(+)}$. This observation suggests that a better assignment is ($24^129^1m^{0,1}$, $24_129_1m_{0,1}$). The 24^129^1 level can interact with 17^1 via both the $m = 0$ and $m = 1$ levels, and so would not directly be the cause of the asymmetry between the 17_1m_1 and 17_1m_0 intensity profiles, which must be due to m-specific interactions; in particular, it can also be seen (Figure 3) that the 17^1m^1 band has an altered shape compared to that of the m^1 origin band (see inset in Figure 1), while the 17^1m^0 band is similar.

The $24^130^1m^2$ assignment would yield a value for 24_1 of 860 cm^{-1}, which would be in excellent agreement with the calculated and previous IR/Raman spectroscopic values. Notwithstanding this, the implication that the contribution is more likely totally-symmetric leads us to favour the 24^129^1 assignment, with $24_129_1m_0$ being attributable to the (687, 1079) cm^{-1} feature. This then yields a value for 24^1 of 514 cm^{-1}, which is in good agreement with the calculated value (Table 2), and a value for 24_1 of 842 cm^{-1}, which is still in reasonable agreement with the quantum chemical and IR/Raman values – particularly considering possible liquid/solvatochromic shifts compared to the present gas-phase value. This would then locate $24_130_1m_2$ at 1061 cm^{-1}, and indeed there is an emission band at that wavenumber, which partially overlaps the $15_1m_{3(+)}$ band. In summary, we assign the 1079 cm^{-1} emission to $24_129_1m_0$ arising from a $24^129^1\ldots17^1$ interaction; the corresponding $24_129_1m_1$ component is likely overlapped by the 14_1 emission. The value of 842 cm^{-1} for D_{24} in the S_0 state is thus adopted.

We now consider the band at (682, 664) cm^{-1}, which is consistent with an assignment to the 21_2m_4 emission. Since only a very faint band is seen at the expected wavenumber for $21_2m_{0,1}$, this cannot be just a FC-active vibtor band. The 21_2m_4 emission is not at quite the expected excitation wavenumber for the $\Delta(v, m) = (0, 0)$ band, expected at 675 cm^{-1}, and although it may arise as a result of emission from other levels, such as 17_1m_1, its intensity does not support this. To be the $\Delta(v, m) = (0, 0)$ band the transition would have to gain intensity from interaction with 17^1m^1 via a $\Delta(v, m) = (3, 3)$ transition, which is plausible, but the inconsistency with the expected excitation position makes us cautious on this point.

A band that appears at (682, 785) cm^{-1} can be associated with the $18^1 29^1 m^2$ excitation, with a $\Delta(v, m)$ = (0, 0) assignment suggested by the absence of other associated vibtor bands, and the good agreement with expected excitation and emission wavenumbers. This is consistent with obtaining intensity from $17^1 m^1$ via a $\Delta(v, m)$ = (3, 3) interaction.

The next band considered is that at (685, 847) cm^{-1}, which can be assigned as involving the $25^1 m^4$ excitation. We suggest that this is a $\Delta(v, m)$ = (0, 0) band, gaining intensity following interaction with $17^1 m^1$ in a $\Delta(v, m)$ = (2, 3) interaction. This assignment yields values for 25^1 of 580 cm^{-1} and for 25_1 of 766 cm^{-1}, both of which are in good agreement with previous and/or calculated values – see Table 2. In our previous paper,[3] we assigned an emission band at 1217 cm^{-1} to $25_1 28_1$ that was seen when exciting via the origin, giving a slightly lower value for 25_1. We now proffer an alternative assignment to that emission band, $22_1 29_1$, giving a value for 22_1 of 980 cm^{-1}.

There are other bands that cannot be associated as vibtor activity from the $17^1 m^{0,1}$ levels, nor are at the correct excitation wavenumbers to be associated with levels that are interacting with the $17^1 m^{0,1}$ levels. We currently assume that these are associated with activity arising from some of the other interacting levels, mostly those that have *e* symmetry. One example is the band at (682, 909) cm^{-1}, which has a possible assignment to a $20_2 m_2$ emission, and is not in the correct excitation position to be a $\Delta(v, m)$ = (0, 0) band.

We now examine the ZEKE spectra in the light of the above assignments, which are presented in Figure 4, and where the main activity was discussed in Ref. 3, and the majority of the bands were assigned to vibtor transitions, $^{+}17^1 m^x$, with the expected pattern of intensities.

Bands assignable to $^{+}26^1 28^1 m^0$ and $^{+}26^1 28^1 m^{3(+)}$ are also present in the ZEKE spectrum when exciting at the wavenumber of $17^1 m^0$ (684 cm^{-1}), and $^{+}26^1 28^1 m^{1,\,2,\,4}$ bands are assignable when exciting at the wavenumber of $17^1 m^1$. As such, this is evidence that there is an interaction between $26^1 28^1$ and 17^1; this seems clearer from the ZEKE spectrum than the 2D-LIF spectrum. Other activity in the ZEKE spectrum is present, but definitive evidence for activity from the other posited interactions deduced from the 2D-LIF spectrum is elusive, because of the overlapping bands and other activity. Thus, it is only by dual consideration of the 2D-LIF and the ZEKE spectra that a more-complete picture of the activity in this region of the $S_1 \leftarrow S_0$ spectrum can be established.

We finish by noting that we assigned some $^{+}25^1 29^1 m^x$ transitions in Ref. 3, but we are now less certain of these, and so omit them here.

4.2 ZEKE spectrum via $17^1 m^{3(+)}$

In the REMPI spectrum shown in Figure 1, there is a weak band to higher wavenumber that is in the correct position to be assigned to $17^1 m^{3(+)}$, and there are a few other weak bands to higher wavenumber. Owing to the weakness of the bands, we have only recorded a ZEKE spectrum via $17^1 m^{3(+)}$, and this is shown in Figure 5. Remarkably, there is significant structure in this spectrum, with the expected[1,2,3] $\Delta m = 3$ bands, $^{+}17^1 m^0$ and $^{+}17^1 m^{6(+)}$ being clearly seen and the $\Delta(v, m) = (0, 0)$ band, $^{+}17^1 m^{3(+)}$ being very weak , and not unambiguously identifiable in this spectrum. Interestingly, there is a significant band assignable as $^{+}26^1 28^1 m^0$ and a band assignable to $^{+}26^1 28^1 m^{6(+)}$ can also be identified to higher wavenumber. These are consistent with a $17^1 m^{3(+)} \ldots 26^1 28^1 m^{3(+)}$ interaction in the S_1 state, mirroring the $17^1 \ldots 26^1 28^1$ interaction. Other bands in the ZEKE spectrum are consistent with reasonable assignments involving totally-symmetric levels, and so attributed to FC activity; however, there are several for which the only possible assignments do not appear to be consistent with the intensity of the bands; we refrain from indicating these at the present time, and those bands are left unassigned in Figure 5.

We saw no clear evidence of activity from other $17^1 m^x$ vibtor levels, such as $17^1 \mathrm{m}^2$ and $17^1 m^4$, in the REMPI or 2D-LIF spectra.

4.3 The $26^1 28^1$ Level

In the LIF spectrum of *m*FT reported by Okuyama et al.,[5] the band we observe at 706 cm^{-1} was assigned as 12^1 (denoted ν_{9b} in that work, using Wilson notation). As Table 2 shows, and in agreement with comments in Ref. 4, this band is far too low in wavenumber for this assignment to be correct, although the value for 12_1 reported in Ref. 5 is close to the calculated (Table 2) and previous IR/Raman values (see the tables and discussion in Ref. 11).

The main features in the 2D-LIF spectrum, Figure 6, are at an emission wavenumber of 1125 cm^{-1} and are concluded to be the $\Delta v = 0$ bands. Comparison with the spectrum of *m*DFB in Figure 1, and the calculated vibrational wavenumbers (Table 2) allows the excitation to be straightforwardly identified as $26^1 28^1$. From the $\Delta(v, m) = (0, 0)$ bands and the established value for 28_1 of 441 cm^{-1}, a value for 26_1 of 684 cm^{-1} is obtained, which is in good agreement with the calculated and IR/Raman values in Table 2; the value is also reasonably close to 12_1, which is likely the reason for the misassignment of the excitation in Ref. 5. In addition, with the value of 253 cm^{-1} for 28^1, then 26^1 may be derived as 453 cm^{-1}, in good agreement with the calculated value (Table 2). Even though the 17_1 emission, when exciting $26^1 28^1$ (Figure 6), is weak, the previous subsection discussed some evidence for a $17^1 \ldots 26^1 28^1$ interaction, and we shall return to this point shortly, when we consider the ZEKE spectra. In Figure 2, it can be seen that when exciting via $26^1 28^1 m^0$, we do not see $m_{3(+)}$, and we also do not see bands corresponding to *e* symmetry torsional levels from $26^1 28^1 m^1$. These observations are consistent with the weakness of the 17_1 emission.

There is another fairly intense band at (706, 968) cm^{-1} in Figure 6. Looking at the activity seen in *m*DFB (see Figure 1), we considered ($25^1 28^1$, $25_1 28_1$) and ($24^1 28^1$, $24_1 28_1$) as possible assignments, however, neither of these agree with the expected band positions for these two bands.

We then considered a possible assignment for this feature of ($25^1 30^1$, $25_1 30_1$), which would be consistent with the values in Table 2 for both the S_0 and S_1 states. This could arise from inherent activity, or via a $26^1 28^1 \ldots 25^1 30^1$ interaction, but which would be $\Delta v = 4$, and so not expected to be strong. Also, given that the $25^1 30^1$ band was not active in the LIF spectrum of *m*DFB,[6] then would be surprising if this were so prominent in *m*FT, unless there were an interaction. Also, examining the spectrum in more detail, we find that we cannot discern the associated vibtor bands that are expected to be associated with the (706, 968) cm^{-1} band, if it were assigned to emission to a vibrational level. Furthermore, if the activity arose from an interaction, then this would give rise to two eigenstates for $m = 0$, namely $25^1 30^1 \mathrm{m}^0 \ldots 26^1 28^1 m^0$ and $26^1 28^1 m^0 \ldots 25^1 30^1 m^0$, and a corresponding pair for $m = 1$. It would then be expected for both of the emissions at 968 cm^{-1} and 1125 cm^{-1} to extend over the same excitation range, which is not the case: the 968 cm^{-1} emission has a narrower extent than the 1125 cm^{-1} emission.

These aspects of the spectrum are what led us to seek another assignment involving a vibtor level: since a vibtor transition would be consistent with the absence of associated vibtor bands mentioned hereinbefore. The appearance and locations of the associated m_2 and the two $m_{3(+)}$ bands associated with the 1125 cm^{-1} emission leads to the conclusion that the interacting vibtor level in the S_1 state needs to be totally symmetric, and so interacts with $26^1 28^1 m^0$, but not $26^1 28^1 m^1$. We currently favour the assignment of the interacting level as $26^1 29^1 m^{3(+)}$, which is consistent with the 968 cm^{-1} emission. That band is at a significantly lower excitation wavenumber than expected for $26^1 29^1 m^{3(+)}$, and we currently assume that its interactions with $26^1 28^1 m^0$ and other levels have produced eigenstates in significantly shifted positions – some vibration-torsion interactions can be sizeable.[4]

Although $26^1 28^1 m^1$ is at the lowest excitation wavenumber, the ordering of the other two states is less clear, but the intensities of the bands suggest $26^1 29^1 m^{3(+)} \ldots 26^1 28^1 m^0$ is the lower wavenumber component of this $\Delta(v, m) = (2, 3)$ interaction. Looking at the REMPI band profile in Figure 2 and Figure

3, and comparing this to the appearance of the origin band (Figure 2), it can be seen that the higher wavenumber side of the $26^1 28^1 m^{0,1}$ feature has an altered shape, and is displaced from the expected $26^1 28^1 m^0$ band position, in line with an m-specific interaction involving $m = 0$. As such, we tentatively assign the S_1 levels between 698 cm^{-1} and 709 cm^{-1} to: $26^1 28^1 m^1$, $26^1 29^1 m^{3(+)} \ldots 26^1 28^1 m^0$, and $26^1 28^1 m^0 \ldots 26^1 29^1 m^{3(+)}$, in order of increasing wavenumber (see Figure 6).

We now consider the ZEKE spectra obtained when exciting across the excitation region containing the $26^1 28^1 m^{0,1}$ bands. These are shown in Figure 7, where six excitation positions have been employed, scanning down to cover the low wavenumber region of the ZEKE spectrum. The appearance of the torsional bands ${}^+m^2$, ${}^+m^4$ and ${}^+m^5$ are characteristic of an intermediate level that involves m^1, and as such support the assignment of the low-wavenumber section of the REMPI band to $26^1 28^1 m^1$; moreover, there are a series of corresponding ${}^+26^1 28^1 m^x$ bands providing definitive evidence for this. Interestingly, each of the latter bands is a doublet, and the other component can be identified as the equivalent ${}^+15^1 m^x$ band. Although these doublets could all be associated with FC activity, we suggest that ${}^+15^1$ and ${}^+26^1 28^1$ are in Fermi resonance in the cation, and that this occurs for each of the associated vibtor levels; this would be reminiscent of the discussed $17^1 \ldots 26^1 28^1$ interaction in the S_1 state.

For the higher-wavenumber excitations, it can be seen that the activity arises from levels associated with $m = 0$, where ${}^+m^{3(+)}$, can be seen at each of the four excitation positions, with ${}^+m^{6(-)}$ and ${}^+m^{6(+)}$ bands also sometimes being identified. It is also clear that the ${}^+26^1 28^1 m^{3(+)}$ band is more intense on the high-wavenumber end of the band, supporting the contribution to the REMPI spectrum here of $26^1 28^1 m^0 \ldots 26^1 29^1 m^{3(+)}$. The intense ZEKE band at 787 cm^{-1} may be assigned to ${}^+26^1 29^1 m^0$, supporting the involvement of $26^1 29^1 m^{3(+)}$ to the S_1 eigenstates with the contribution from $26^1 29^1 m^{3(+)} \ldots 26^1 28^1 m^0$ being located in the centre of the REMPI band, consistent with the 2D-LIF spectrum discussed earlier. The ZEKE band at 802 cm^{-1} appears to arise from a Fermi resonance in the cation: ${}^+26^1 29^1 m^0 \ldots 18^1 29^1 m^{3(-)}$, and its intensity follows that of the 787 cm^{-1} band.

It is also clear that at the higher excitation wavenumbers, we see bands that are assignable to ${}^+20^1 21^1 m^{3(+)}$ and ${}^+20^1 21^1 m^{6(+)}$, which would be consistent with $Y^1 21^1 m^0$ activity, even though the corresponding 2D-LIF bands are weak (see Figure 3). Unambiguous identification of the *e* symmetry ${}^+20^1 21^1 m^x$ bands when exciting at the lower wavenumbers, where $Y^1 21^1 m^1$ would be expected, is less straightforward, owing to the large amount of structure in the spectrum.

In summary, the strong activity of the ${}^+17^1 m^x$ bands, taken together with the complementary activity seen when exciting via $17^1 m^{0,1}$, is highly suggestive of a $17^1 \ldots 26^1 28^1$ interaction occurring for both m

= 0 and 1 levels, with a further $26^1 28^1 m^0 \ldots 26^1 29^1 m^{3(+)}$ interaction occurring. The evidence for the $17^1 \ldots 26^1 28^1$ interaction is much clearer in the ZEKE spectra than it is in the 2D-LIF spectra; however, taken together, this is persuasive.

4.4 The 27^2, $18^1 21^1$ and $X^1 21^1$ Levels

In the LIF spectrum of *m*FT reported by Okuyama et al.,[5] a band at 746 cm^{-1} was assigned as 13^1 (denoted ν_{18b} in Wilson notation, in that work), which we find is at 741 cm^{-1}. As Table 2 shows, and in agreement with comments in Ref. 4, this band is far too low in wavenumber for this assignment to be correct, although the value for 13_1 reported in Ref. 5 is close to the calculated (Table 2) and previous IR/Raman values (see tables and discussion in Ref. 11).

In the 2D-LIF spectrum in Figure 8, the most intense features occur across a range of emission wavenumbers of 1104–1122 cm^{-1} – see the inset to Figure 8. Comparison with the spectrum of *m*DFB (see Figure 1), and the calculated vibrational wavenumbers (Table 2), allows the main excitation to be assigned as 27_2. The emission band (1114 cm^{-1}) at lower excitation wavenumber is straightforwardly assignable as $27_2 m_1$, but it is noteworthy that there are two such bands to higher excitation wavenumber, and the lower of these emission bands (1110 cm^{-1}) is the more intense. In addition, the other band is displaced to slightly higher emission wavenumber (1116 cm^{-1}) than $27_2 m_1$. As such, we conclude that at the higher excitation wavenumber, the lower-wavenumber of the two emission bands mainly arises from $27_2 m_0$, and is moved to lower emission wavenumber, owing to an interaction in the S_0 state (see inset to Figure 8). Looking at the possibilities for a totally-symmetric vibtor level, we identify the interacting level as $19_1 27_1 m_{3(-)}$ – a $\Delta(v, m) = (2,3)$ interaction; this then gives rise to the pair of observed bands. Interestingly, a similar pattern of emission bands appears in the range 1231–1245 cm^{-1}, which is interpreted as a similar interaction between $26_1 27_1 m_0$ and $19_1 26_1 m_{3(-)}$ – see Figure 8. The observed wavenumbers are consistent with the calculated values (Table 2) and those derived from the ($26^1 28^1$, $26_1 28_1$) band discussed in the previous subsection.

The REMPI (Figure 1) or integrated 2D-LIF (Figure 8) band profiles are each different from those of the origin, suggesting that other activity is present at this wavenumber, and this is also demonstrated by the 2D-LIF spectrum in Figure 8. Bands associated with $18_1 21_1$ and $19_1 21_1$, are clearly seen in the 2D-LIF spectrum, and are unlikely to simply be due to FC activity. Comparison with the values in Table 2, together with the similarity of the pattern of 2D-LIF bands seen when exciting 18^1 and X^1 – see Ref. 2 – makes it clear that these are $\Delta v = 0$ bands arising from $18^1 21^1$ and $X^1 21^1$ excitations. At around 705 cm^{-1}, the excitation spectra reported in Ref. 2 suggest we should see the $Y^1 21^1$ band also whose emission features are at ~736 cm^{-1}. These are seen to be very weak (Figure 6) although the corresponding ZEKE bands in Figure 7 are more prominent; it may also be that the $18^1 21^1$ and $X^1 21^1$ excitations are interacting weakly with 27^2, and hence gaining some intensity from it.

Since we did not observe pure torsional emission bands when exciting via $26^1 28^1$, we may not expect to see these via 27^2; however, we do see a weak $m_{3(+)}$ band at the corresponding excitation energy (see Figure 2) and so we hypothesise that this arises from activity associated with the $18^1 21^1$ and $X^1 21^1$ levels, which are made up of totally-symmetric vibrations. We do not see any *e* symmetry pure torsional emission bands arising from $27^2 m^1$, but these may simply be too weak to see.

ZEKE spectra have been recorded at four positions across the feature that includes the $27^2 m^{0,1}$ transitions, and these are shown in Figure 9. It is immediately apparent that two of the spectra are associated with the $m = 1$ component, as ascertained from the $^+m^1$, $^+m^2$, $^+m^4$ and $^+m^5$ bands, while the other two cover $m = 0$, as ascertained from the $^+m^{3(+)}$, $^+m^{6(-)}$ and $^+m^{6(+)}$ bands (with the $^+m^0$ band being barely discernible).[1,2,3] The high-wavenumber region of each spectrum shows the corresponding $^+27^2 m^x$ bands. It is notable in all spectra that there is significant additional structure than the expected bands, and this is particularly the case for those corresponding to $m = 1$ where there are numerous bands, including at low wavenumber.

As noted, we expect some activity from $18^1 21^1$ and $X^1 21^1$ in this region, and indeed bands supporting this activity are present, although these are more difficult to identify definitively in the $m = 1$ case. In previous work on *m*FT,[1,2,3] *p*FT, [8,17,18,19,20,21,22,23] and *N*-methylpyrrole (NMP),[24] we have noted how the low-wavenumber region of ZEKE spectra can often give strong hints as to the assignment, since bands assignable to torsions, vibrations or vibtors that form part of combination bands are often seen. The low-wavenumber region of the spectra in Figure 9 suggests that there is little interaction involving the $27^2 m^0$ level, but significant interactions involving $27^2 m^1$, in line with the activity seen in these spectra; identification of explicit interactions in this case has not, however, been possible, except the interactions with $X^1 21^1$ and $18^1 21^1$. As mentioned earlier, the significant change in the torsional potential upon ionization causes each contributing level to give rise to a number of ZEKE bands and this makes a full assignment "challenging". As such, we have restricted ourselves to highlighting the main contributions, as discussed above and labelled in Figure 9.

Finally, we comment on a weak excitation feature at 727 cm^{-1} that appears in the REMPI spectrum (Figure 1), as well as in the integrated 2D-LIF spectrum (top of Figure 2) – marked with an obelus in both cases. It can be seen from the 2D-LIF spectrum in Figure 2 that there are some weak features associated with this band, for example at (727, 902) cm^{-1} and (725, 930) cm^{-1}. Possible, tentative $\Delta(v, m) = 0$ assignments of the first feature is ($25^1 m^5$, $25_1 m_5$), while two possible $\Delta(v, m) = 0$ assignments for the second one are (26^1m^7, 26_1m_7) and ($20^128^1m^{3(-)}$, $20_128_1m_{3(-)}$), with the transitions involving *e* symmetry levels can each gain intensity via interaction with one or more of 27^2m^1, $X^121^1m^1$, $18^121^1m^1$, which would be Δ(*v*, *m*) = (3, 6); while the transition involving the *a*′ symmetry levels can gain intensity from interacting with one or more of 27^2m^0, $X^121^1m^0$, $18^121^1m^0$, which would be Δ(*v*, *m*) = (4, 3). None of these interactions is expected to be especially strong, in keeping with the weak nature of the excitation feature. Other weak features in the REMPI and integrated LIF spectra are not considered further here.

5. Further Remarks and Conclusions

In the present work, we have investigated a ~150 cm^{-1} region of the $S_1 \leftarrow S_0$ REMPI spectrum of *m*FT. By recording 2D-LIF and ZEKE spectra, we have gained significant insight into the S_1 levels that give rise to this spectrum; a summary of the transitions discussed are presented in Table 3. In addition, these spectra have revealed interactions in the S_0 and D_0^+ states. Even with these detailed spectra, it is clear that unpicking all of the interactions is complicated, although we feel confident that we have identified the main interactions. In the S_1 state, we have identified that the main *m*-specific interactions for the 17^1 level are via the *m* = 1 component, while for 26^128^1, the main interaction is via the *m* = 0 component. Furthermore, there is evidence for a Fermi resonance between 17^1 and 26^128^1 in the S_1 state, but this occurs in tandem with the $26^128^1m^0\ldots26^129^1m^{3(+)}$ interaction, and other interactions involving 17^1m^1. As a consequence, providing a comprehensive and quantitative picture of the interactions is difficult. The ZEKE spectrum of $17^1m^{3(+)}$ also supports the $17^1\ldots26^128^1$ Fermi resonance, with evidence also presented for the corresponding interaction for the vibtor levels: $17^1m^{3(+)}\ldots26^128^1m^{3(+)}$. Of course, such interactions are expected for all such vibtor levels[4] (in the same way as they would be expected for vibrational combinations), and notably will be occurring for the corresponding m^0 and m^1 levels; this means that, to first order, all vibtor levels will shift in sync as a result of vibrational interactions, such as a Fermi resonance. As a particular example, the ZEKE spectra in Figure 7 reveal that there is likely a $^+15^1\ldots^+26^128^1$ interaction that occurs for each of the observed vibtors for a particular *m* value. The caveat to this is that any particular vibtor level may (also) be undergoing additional level-specific interactions, of the type identified for torsional and vibtor levels by Stewart et al.[4] As one example, we commented on the $^+26^129^1m^0\ldots^+18^129^1m^{3(-)}$ interaction seen in the ZEKE spectra presented in Figure 7, recorded at the higher excitation wavenumbers.

To slightly higher wavenumber is the 27^2 transition, and it is found that there are likely some weak Δ*v* = 4 interactions with 18^121^1 and X^121^1 in the S_1 state; however, the most significant interaction is $27_2\ldots19_127_1m_{3(-)}$ in the S_0 state, and a corresponding $26_127_1\ldots19_126_1m_{3(-)}$ interaction is also seen.

We have commented here, and in previous work,[2,3] that there are complications in the interpretation of the spectra of *m*FT, with the strong cross-activity in the 2D-LIF spectra of 15^1 and 17^1, even though these two vibrations are not obviously Duschinsky mixed.[3] We have also noted the complications posed by the non-$\Delta(v, m) = (0, 0)$ activity that occurs upon ionization; this, coupled with the various interactions in the S_1 state leads to some ZEKE spectra showing a cornucopia of activity, and some 2D-LIF spectra also show a range of weaker activity. Considering also that various other higher-order interactions are likely occurring, is it probably a fruitless task to try and assign every weak band in the spectra. Taking this pragmatic view, we have tried to restrict ourselves to reporting the main interactions, while giving a flavour of the more-complicated underlying picture.

We highlight that the region of the excitation spectrum considered here corresponds to relatively low internal energies, and so the complexity is quite surprising, particularly as the density of states is still quite low,[3] probably only a few levels per cm^{-1} at most. However, the lower symmetry of *m*FT compared to other molecules, such as *p*DFB[18,25,] *p*FT[8,16,17,18,19,20,21,22,23] and NMP[24] gives more possibilities for interaction, especially those corresponding to odd-*m* vibtor levels, which all have the same *e* symmetry in the G_6 MSG.[3] Although only limited wavenumber region of the excitation spectrum of the *m*-chlorotoluene molecule have been studied,[2,26] evidence for such interactions were also seen in that molecule. The serendipitous nature of IVR at low wavenumber was discussed in Ref. 18 in relation to *para*-disubstituted benzenes, and the present results, in tandem with those in Refs. 1, 2, 3, particularly the latter, confirm that this is also the case in *m*FT.

In summary, even at the low internal wavenumber considered herein, a rather complicated picture of interacting levels emerges. However, a great deal of insight is possible using a partnership of fluorescence and ionization spectroscopies. Of course, for the vast majority of larger (bio)molecules, the symmetry will drop further, opening up more coupling routes.

Acknowledgements

We are grateful to the EPSRC for funding (grant EP/L021366/1). The EPSRC and the University of Nottingham are thanked for studentships to D.J.K. and A.R.D. Continuing discussions on vibration-torsional couplings with Warren Lawrance and Jason Gascooke (Flinders University) are gratefully acknowledged.

Data Availability Statement

The data that support the findings of this study are available from the corresponding author upon reasonable request.

Table 1: Correspondence of the C_s point group symmetry classes with those of the G_6 molecular symmetry group. Also indicated are the symmetries of the D_i vibrations and the different pure torsional levels.[a]

C_s	G_6	D_i[b]	m
a'	a_1	D_1–D_{21}	0, 3(+), 6(+), 9(+)
a''	a_2	D_{22}–D_{30}	3(-), 6(-), 9(-)
	e		1, 2, 4, 5, 7, 8

[a] Symmetries of vibtor levels can be obtained by combining the vibrational symmetry (in G_6) with those of the pure torsional level, using the C_{3v} point group direct product table.

[b] The D_i labels are described in Ref. 11, where the vibration mode diagrams can also be found.

Table 2: Calculated and experimental wavenumbers (cm^{-1}) for the vibrations of *m*-difluorobenzene and *m*-fluorotoluene.

D_i	C_{2v} [a]		S$_0$				S$_1$				D$_0^+$	
			*m*DFB		*m*FT		*m*DFB		*m*FT		*m*FT	
			Calc[b]	Expt[c]	Calc[b]	Expt[c]	Calc[b]	Expt[c]	Calc[d]	Expt[e]	Calc[f]	Expt[g]
		a' (a_1)[h]										
D_1	1	a_1	3122	3095	3107	[3081]	3157		3128		3119	
D_2	2	a_1	3116	3086	3088	[3060]	3141		3114		3107	
D_3	21	b_2	3112	3086	3086		3115		3123		3111	
D_4	3	a_1	3090		3072		3113		3084		3092	
D_5	4	a_1	1597	1611	1578	[1595]	1529	(1519)	1512		1541	1569
D_6	22	b_2	1592	1613	1603	[1623]	1480		1494		1490	
D_7	23	b_2	1475	1490	1479	[1492]	1375		1392		1444	
D_8	5	a_1	1439	1435	1420	[1460]	1378	(1346)	1363		1385	
D_9	24	b_2	1304	1337	1302	1294	1435		1411		1356	
D_{10}	6	a_1	1255	1277	1239	1254	1250		1243		1299	1290
D_{11}	25	b_2	1252	1292	1271	1271	1228	1267	1252	1260	1258	1275
D_{12}	26	b_2	1145	1157	1148	1132	1118	1145	1122	[i]	1143	
D_{13}	27	b_2	1102	1120	1126	1115	1094	(1206)	1113	[i]	1101	
D_{14}	7	a_1	1058	1068	1071	1081	995	998	1023		1074	
D_{15}	8	a_1	994	1012	988	1004	958	966	958	965	997	984
D_{16}	28	b_2	941	956	912	930	883	936	866	840	873	874
D_{17}	9	a_1	726	739	720	731	698	701	685	684	700	710
D_{18}	10	a_1	514	522	519	525	437	442	459	460	509	510
$D_{19(\mathrm{X})}$	29	b_2	502	513	505	512	439	444	448	457	410	415
$D_{20(\mathrm{Y})}$	30	b_2	467	477	435	445	462	468	410	420	442	456
D_{21}	11	a_1	320	329	285	294	314	317	281	285	290	298
		a'' (a_2)[h]										
D_{22}	15	b_1	963	957	967	980	719	(581)	760		988	
D_{23}	12	a_2	871	876	886	[886]	723	672	705		916	
D_{24}	16	b_1	856	857	859	842[j]	362	480	501	514[j]	855	
D_{25}	17	b_1	767	771	773	766	500	(479)	575	580	787	780
D_{26}	18	b_1	671	680	683[k]	683	458	422	468	453	592	592
D_{27}	13	a_2	597	603	557	557	400	369	377	371	514	517
D_{28}	19	b_1	455	454	443	441	239	260	241	253	373	380
D_{29}	14	a_2	239	252	236	237	187	176	184	174	190	190
D_{30}	20	b_1	222	227	199	201	97	127	122	128	167	169

[a] Labels discussed in Ref. 11, where mode diagrams are presented. The values in parentheses are the Mulliken C_{2v} numbers used in Ref. 6 for *m*DFB. For D_{19} and D_{20} the motions are very mixed in the S_1 state of *m*FT, as discussed in Ref. 2, and are denoted therein as D_X and D_Y respectively.

[b] B3LYP/aug-cc-pVTZ, scaled by 0.97 – see Ref. 3.

[c] S_0 values are those obtained in jet-cooled expansion experiments or, when such values are not available, those from IR/Raman studies of liquids or solutions are given in square brackets – see Refs. 3 and 11. For the S_1 state, values that were deemed uncertain in Ref. 6 are given in parentheses.

[d] TD-B3LYP/aug-cc-pVTZ, scaled by 0.97. These values have been recalculated here, and are almost identical to those reported in Ref. 3, but where the four highest wavenumber values were omitted. (These values are also close to the TD-B3LYP/cc-pVTZ values presented in Ref. 4, but several of the values may be seen to be sensitive to the addition of diffuse functions to the basis set.)

[e] Gas phase values taken from Refs. 1,2,3,4 and the present work, in some cases confirming a value reported in Ref. 5.

[f] UB3LYP/aug-cc-pVTZ, scaled by 0.97; $\langle S^2 \rangle = 0.76$.[3]

[g] Values taken from Refs. 1,2,3 and the present work.

[h] Symmetry label in the C_s point group, with G_6 molecular symmetry group label in parentheses.

[i] Experimental values for these two vibrations were reported in Ref. 5, but have been concluded to have been misassigned.[4]

[j] Value obtained in the present work from the assignment of the ($24^1 29^1$, $24_1 29_1$) emission – see text.

[k] Slightly different values are obtained from the $26_1 28_1$ and $26_1 27_1$ bands; the average value is given here.

Table 3: Summary of transitions

Excitation wavenumber/ cm^{-1}	Main contributor[a]
681	17^1m^1
682	(21^2m^4 / $18^129^1m^2$)
684	17^1m^0
685	25^1m^4
687	$24^129^1m^0$
702	$26^128^1m^1$
704	$26^129^1m^{3(+)}$…$26^128^1m^0$
706	$26^128^1m^0$…$26^129^1m^{3(+)}$
727	(25^1m^5/ 26^1m^7/ $20^128^1m^{3(-)}$)
737	$X^121^1m^1$
738	27^2m^1
740	$18^121^1m^1$ / $X^121^1m^0$
742	27^2m^0
745	$18^121^1m^0$
773	$17^1m^{3(+)}$
795	$26^128^1m^{3(+)}$

[a] Interactions between a number of states of the same symmetry are expected and are discussed in the text. Significant interactions in the S_1 state are indicated by "…". A solidus (/) indicates overlapping contributions. See Table 1 and Table 2 for symmetries of vibrational and torsional levels. Tentative assignments are indicated by parentheses.

Figure Captions

Figure 1: REMPI spectrum of (a) *m*-fluorotoluene; and (b) *m*-difluorobenzene. The REMPI assignments of *m*-fluorotoluene are discussed in the text, while those of *m*-difluorobenzene were presented and discussed by Graham and Kable for their LIF spectrum,[6] and commented on in Ref. 3. In the insert, top right, we show the origin bands on the same wavenumber scale, to allow band shapes to be compared – see text. The band marked with an obelus in the top trace is discussed in the text, and the corresponding band is also indicated in the integrated 2D-LIF spectrum at the top of Figure 2.

Figure 2: The top trace, which can be seen to resemble closely the REMPI spectrum of *m*FT in Figure 1(a), is the vertically-integrated version of the whole 2D-LIF spectrum. Below this, two sections of the 2D-LIF spectrum are presented: the top section shows the low-wavenumber emission region; the bottom section shows the main $\Delta(v, m) = (0, 0)$ activity. In the integrated trace at the top, the main contributions are indicated – see text for further discussion of interactions. Only selected main emission assignments are given on the 2D-LIF sections, with further assignments discussed in the text and shown on Figure 3, Figure 6, and Figure 8. The band marked with an obelus in the integrated 2D-LIF trace is discussed in the text, and the corresponding band is also indicated in the REMPI spectrum of mFT at the top of Figure 2; it may be seen that there are weak features in the 2D-LIF spectrum, particularly evident in the 850–1150 cm^{-1} emission wavenumber range.

Figure 3: Section of the 2D-LIF spectrum corresponding to the $17^1m^{0,1}$ region. The intensity scale has been adjusted from that in Figure 2 to emphasise some of the key weaker features. The top trace is the vertically-integrated version of the 2D-LIF spectrum, with the main excitation assignments shown; these and the main emission assignments are discussed further in the text. The colouring of some labels is merely for clarity.

Figure 4: ZEKE spectra recorded at the indicated excitation positions across the $17^1m^{0,1}$ region. Key assignments are indicated and discussed further in the text. The preceding superscripted "+" is omitted from the assignments to avoid congestion. Each spectrum has been normalized to the most intense band. The colouring of some labels and combs is merely for clarity.

Figure 5: ZEKE spectrum recorded via $17^1m^{3(+)}$. Key assignments are indicated and discussed further in the text. The preceding superscripted "+" is omitted from the assignments to avoid congestion. There

are several sizeable bands for which there are possible assignments, but these are troublesome owing to their unexpected intensity; as such, we refrain from indicating these at the present time. We have indicated the expected position for $^{+}17^{1}m^{3(+)}$ with a dashed line, as there is no definitive band at this position.

Figure 6: Section of the 2D-LIF spectrum corresponding to the $26^{1}28^{1}m^{0,1}$ region. The intensity scale has been adjusted from that in Figure 2 to emphasise some of the key weaker features. The top trace is the vertically-integrated version of the 2D-LIF spectrum, with the main excitation assignments shown; these and the main emission assignments are discussed further in the text. The colouring of some labels is merely for clarity.

Figure 7: ZEKE spectra recorded at the indicated excitation positions across the $26^{1}28^{1}m^{0,1}$ region. Key assignments are indicated and discussed further in the text. The preceding superscripted "+" is omitted from the assignments to avoid congestion. Each spectrum has been normalized to the most intense band. The colouring of some labels and combs is merely for clarity.

Figure 8: Section of the 2D-LIF spectrum corresponding to the $27^{2}m^{0,1}$ region. The intensity scale has been adjusted from that in Figure 2 to emphasise some of the key weaker features. The top trace is the vertically-integrated version of the 2D-LIF spectrum, with the main excitation assignments shown; these and the main emission assignments are discussed further in the text. In the inset, top right, and expanded view is shown of the 27_{2} emission region, indicating the presence of a Fermi resonance in the S_0 state – see text for further comment.

Figure 9: ZEKE spectra recorded at the indicated excitation positions across the $27^{2}m^{0,1}$ region. Key assignments are indicated and discussed further in the text. The preceding superscripted "+" is omitted from the assignments to avoid congestion. Each spectrum has been normalized to the most intense band. The colouring of some labels and combs is merely for clarity.

Figure 1

a) *m*-fluorotoluene

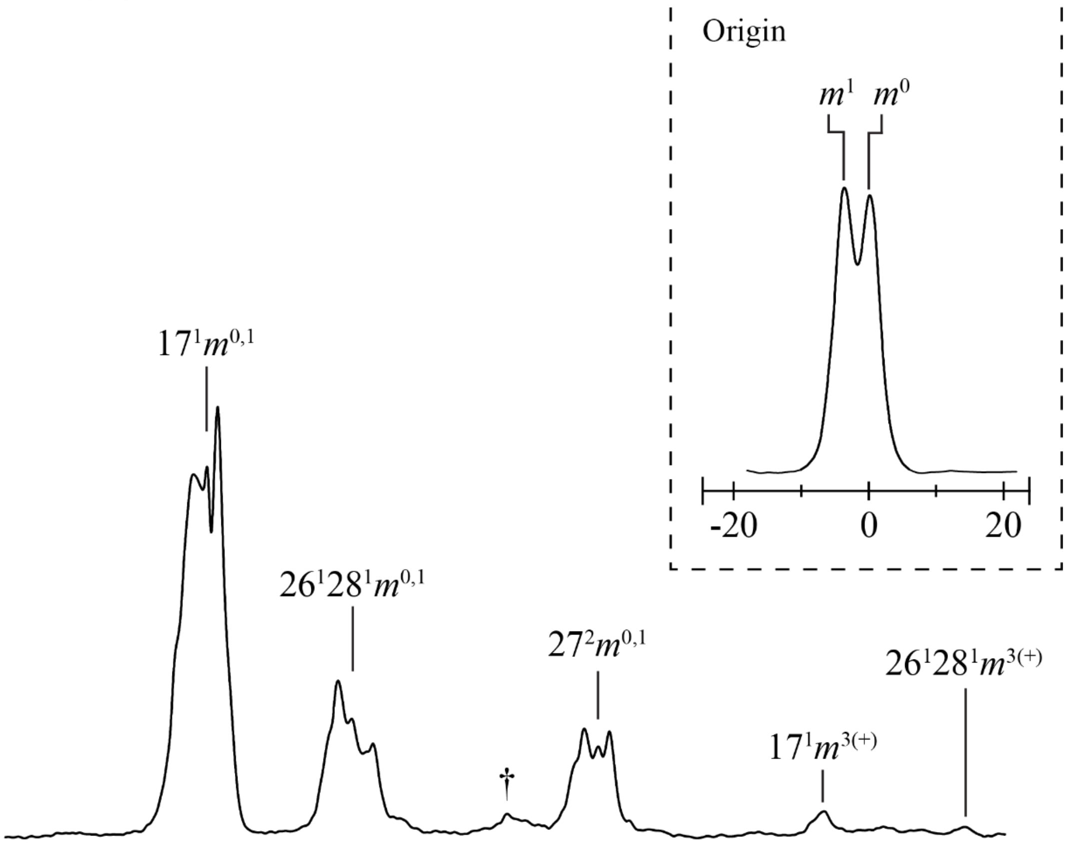

b) *m*-difluorobenzene

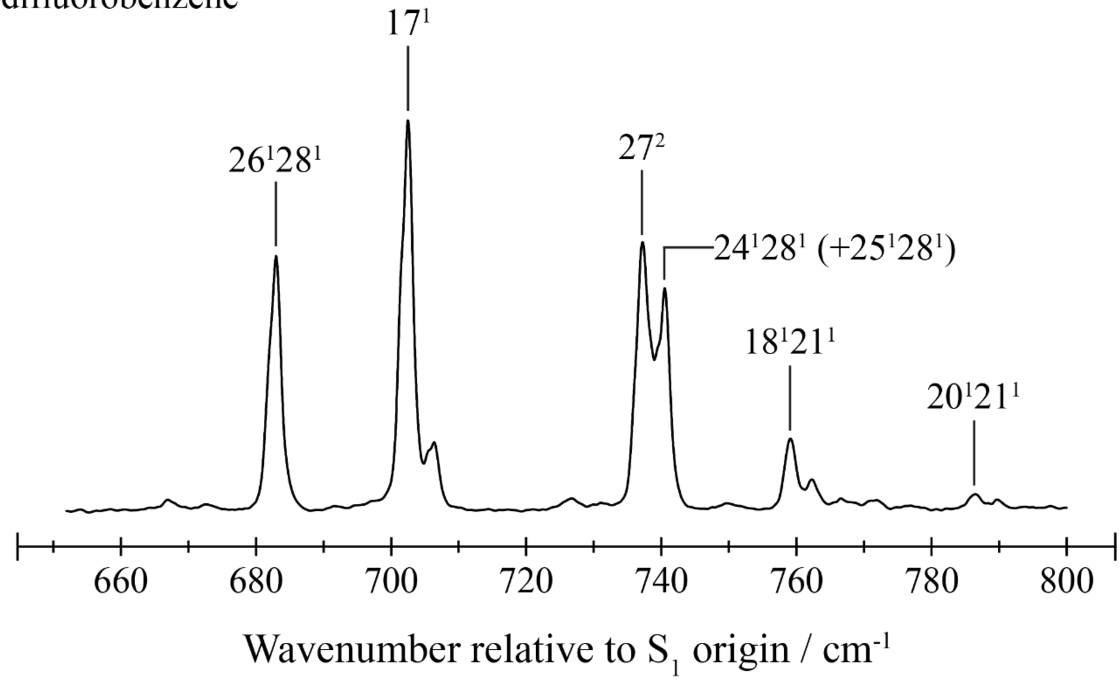

Figure 2

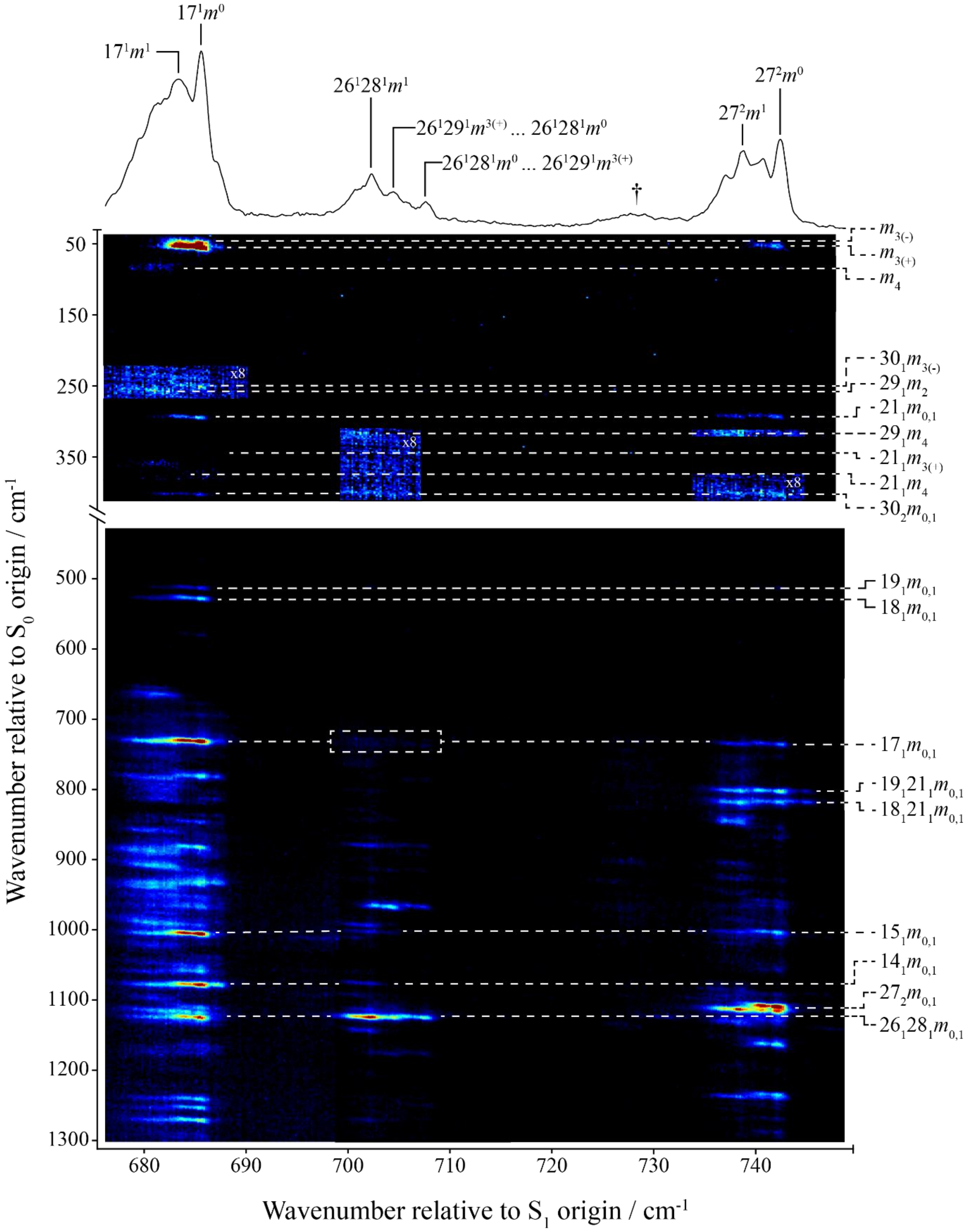
17^1m^0
17^1m^1
$26^128^1m^1$
$26^129^1m^{3(+)}$ ... $26^128^1m^0$
$26^128^1m^0$ ... $26^129^1m^{3(+)}$
†
27^2m^1
27^2m^0
$m_{3(-)}$
$m_{3(+)}$
m_4
$30_1m_{3(-)}$
29_1m_2
$21_1m_{0,1}$
29_1m_4
$21_1m_{3(+)}$
21_1m_4
$30_2m_{0,1}$
x8
x8
x8
$19_1m_{0,1}$
$18_1m_{0,1}$
$17_1m_{0,1}$
$19_121_1m_{0,1}$
$18_121_1m_{0,1}$
$15_1m_{0,1}$
$14_1m_{0,1}$
$27_2m_{0,1}$
$26_128_1m_{0,1}$
Wavenumber relative to S_0 origin / cm^{-1}
50
150
250
350
500
600
700
800
900
1000
1100
1200
1300
680
690
700
710
720
730
740
Wavenumber relative to S_1 origin / cm^{-1}

Figure 3

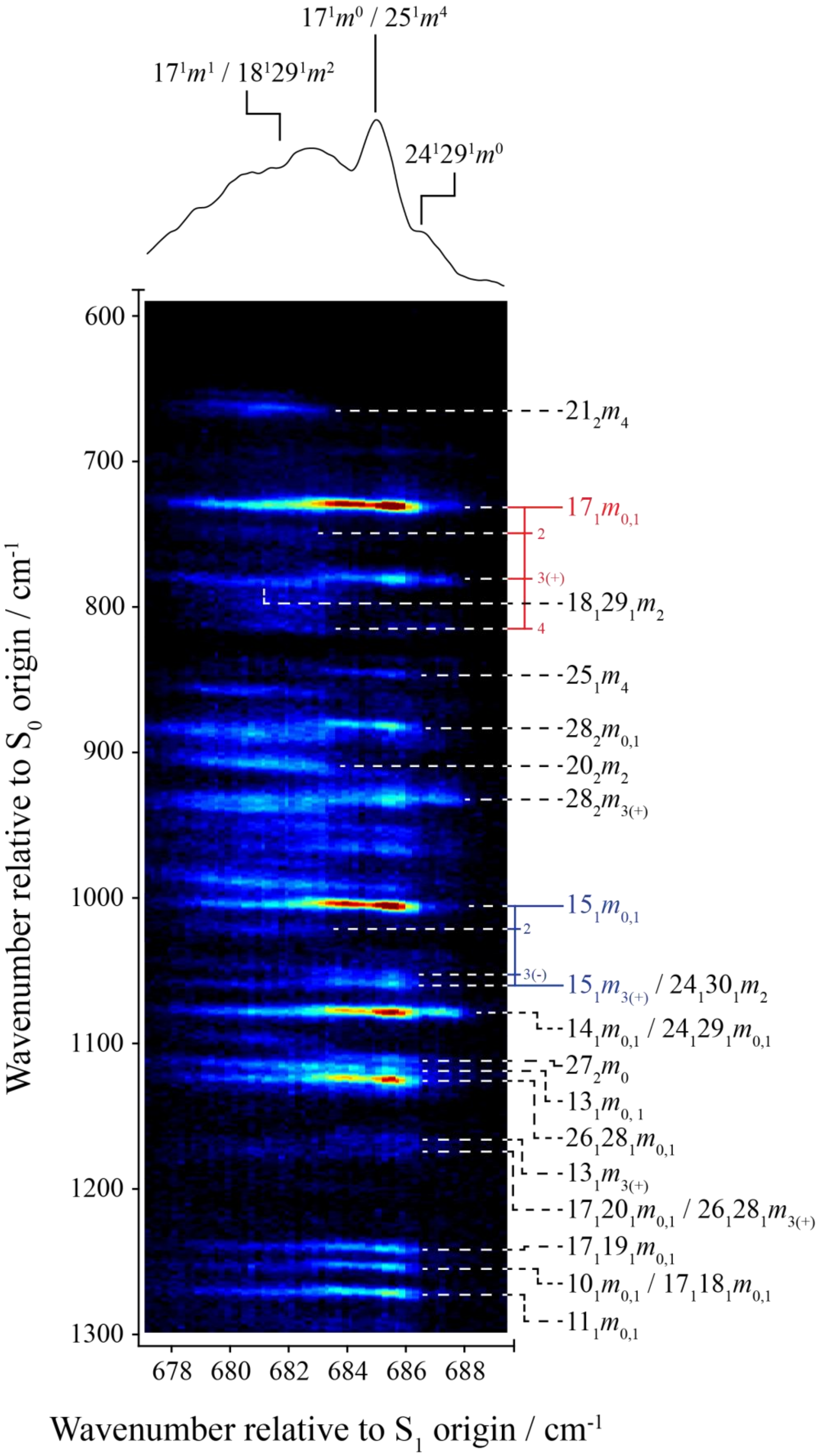

17^1m^0 / 25^1m^4
17^1m^1 / $18^129^1m^2$
$24^129^1m^0$
600
700
800
900
1000
1100
1200
1300
Wavenumber relative to S_0 origin / cm^{-1}
21_2m_4
$17_1m_{0,1}$
2
3(+)
4
$18_129_1m_2$
25_1m_4
$28_2m_{0,1}$
20_2m_2
$28_2m_{3(+)}$
$15_1m_{0,1}$
2
3(-)
$15_1m_{3(+)}$ / $24_130_1m_2$
$14_1m_{0,1}$ / $24_129_1m_{0,1}$
27_2m_0
$13_1m_{0,1}$
$26_128_1m_{0,1}$
$13_1m_{3(+)}$
$17_120_1m_{0,1}$ / $26_128_1m_{3(+)}$
$17_119_1m_{0,1}$
$10_1m_{0,1}$ / $17_118_1m_{0,1}$
$11_1m_{0,1}$
678
680
682
684
686
688
Wavenumber relative to S_1 origin / cm^{-1}

Figure 4

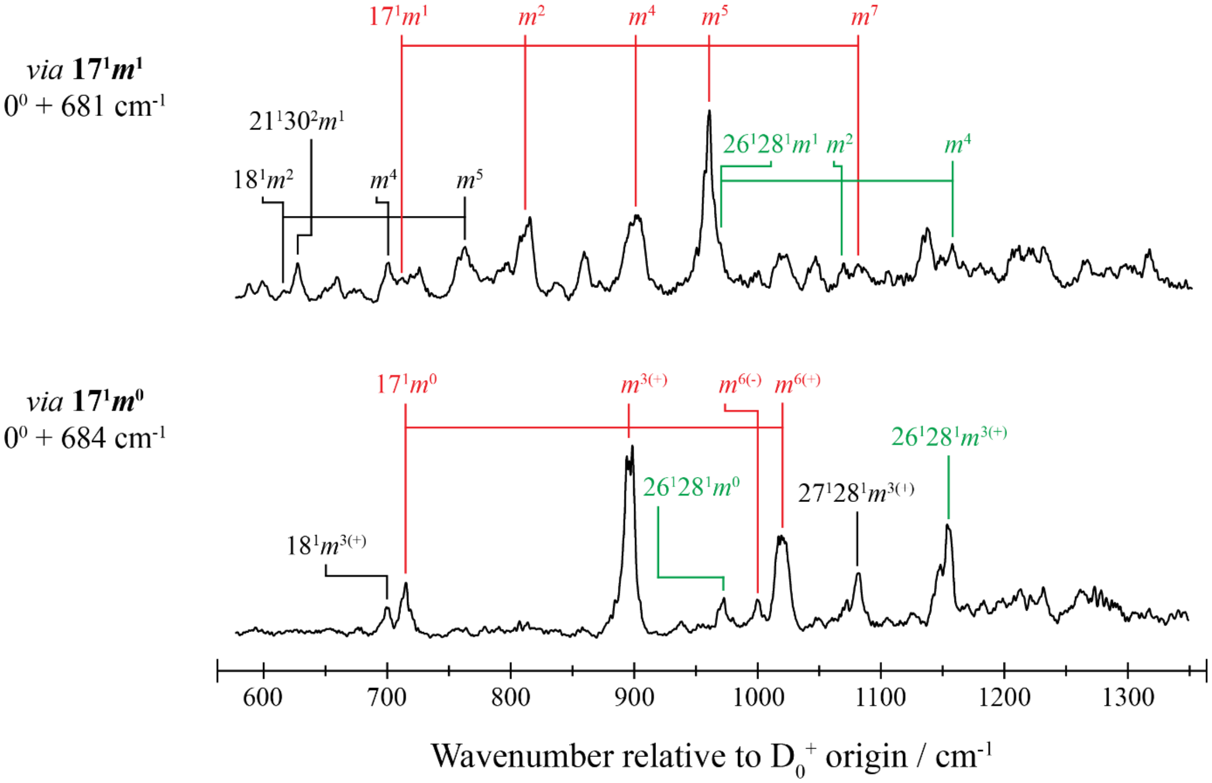
via $\mathbf{17^1}\boldsymbol{m^1}$
0^0 + 681 cm^{-1}
17^1m^1
m^2
m^4
m^5
m^7
$21^130^2m^1$
18^1m^2
m^4
m^5
$26^128^1m^1$
m^2
m^4
via $\mathbf{17^1}\boldsymbol{m^0}$
0^0 + 684 cm^{-1}
17^1m^0
$m^{3(+)}$
$m^{6(-)}$
$m^{6(+)}$
$26^128^1m^{3(+)}$
$26^128^1m^0$
$27^128^1m^{3(-)}$
$18^1m^{3(+)}$
600
700
800
900
1000
1100
1200
1300
Wavenumber relative to D_0^+ origin / cm^{-1}

Figure 5

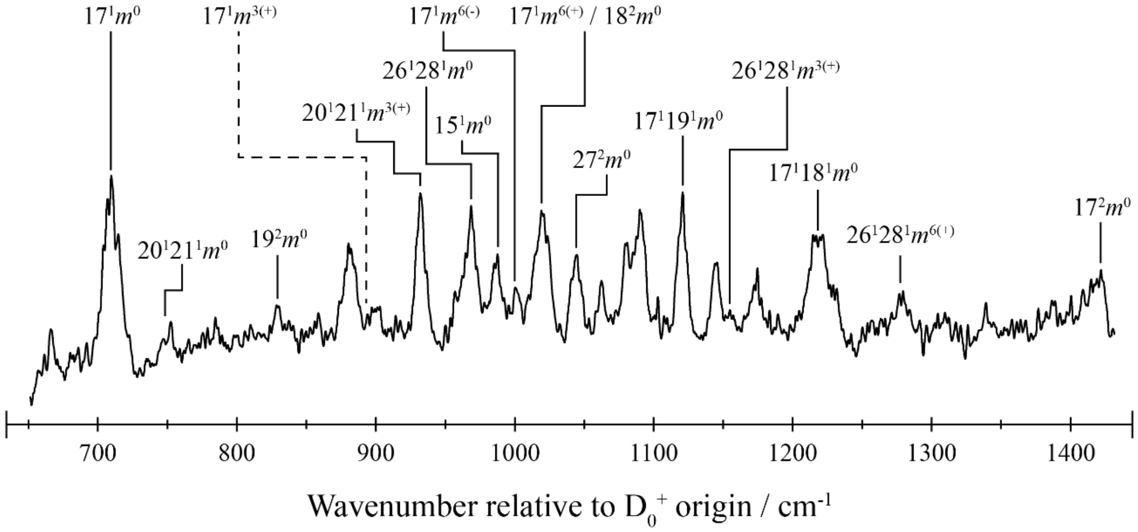

via $\mathbf{17^1}\boldsymbol{m}^{\mathbf{3(+)}}$
$0^0 + 773\ \mathrm{cm}^{-1}$

Figure 6

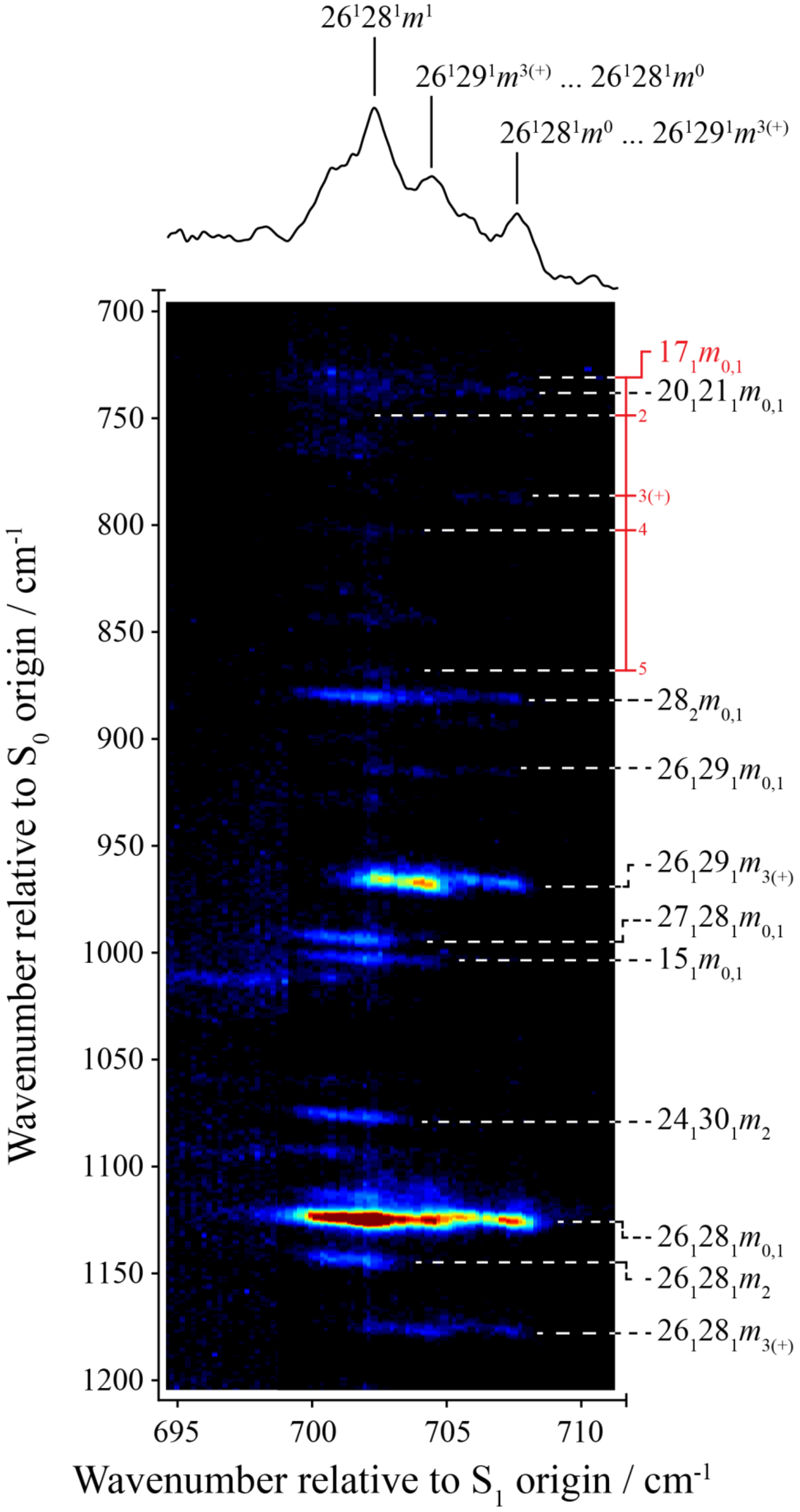
$26^1 28^1 m^1$
$26^1 29^1 m^{3(+)}$ ... $26^1 28^1 m^0$
$26^1 28^1 m^0$ ... $26^1 29^1 m^{3(+)}$
700
750
800
850
900
950
1000
1050
1100
1150
1200
Wavenumber relative to S_0 origin / cm^{-1}
695
700
705
710
Wavenumber relative to S_1 origin / cm^{-1}
$17_1 m_{0,1}$
$20_1 21_1 m_{0,1}$
2
3(+)
4
5
$28_2 m_{0,1}$
$26_1 29_1 m_{0,1}$
$26_1 29_1 m_{3(+)}$
$27_1 28_1 m_{0,1}$
$15_1 m_{0,1}$
$24_1 30_1 m_2$
$26_1 28_1 m_{0,1}$
$26_1 28_1 m_2$
$26_1 28_1 m_{3(+)}$

Figure 7

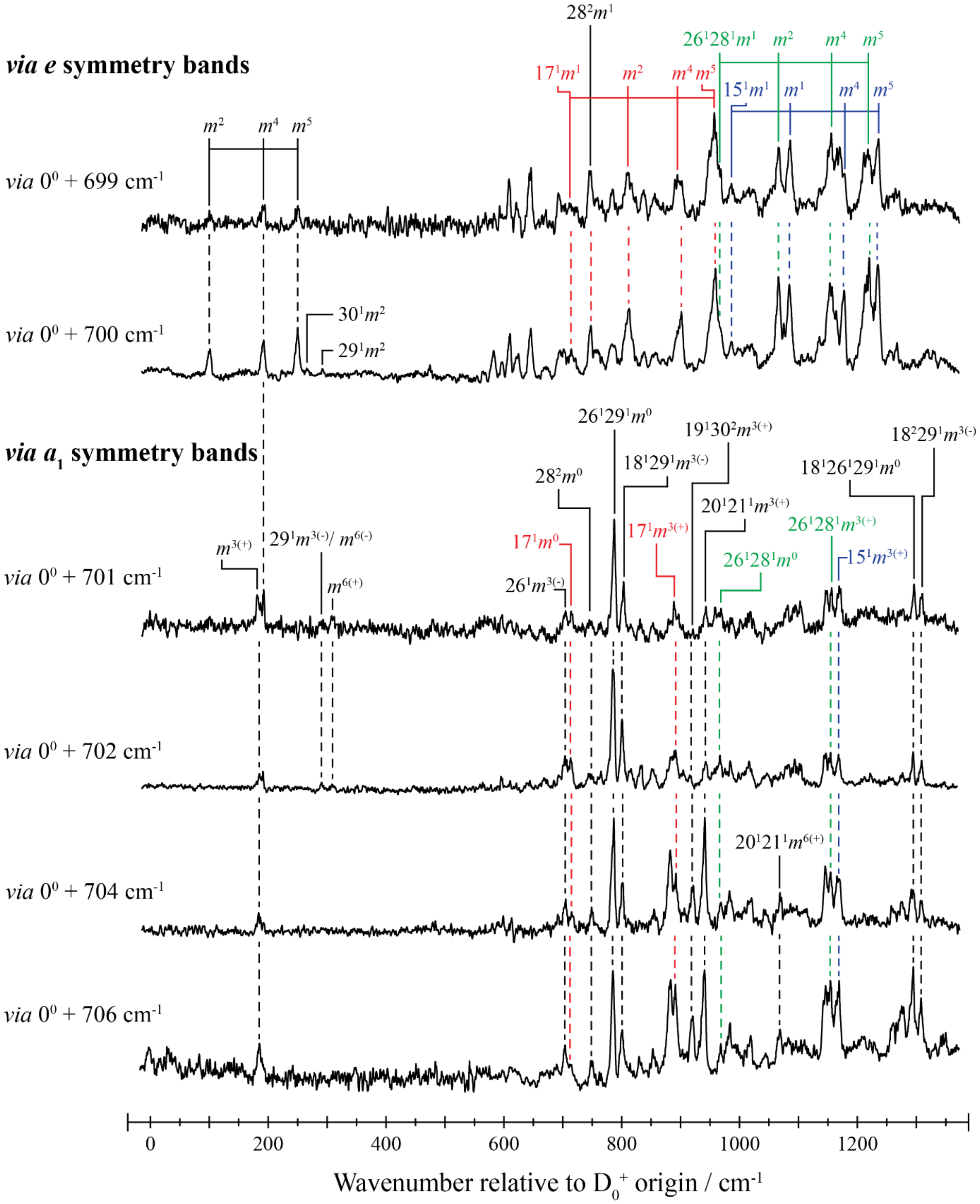
via e symmetry bands
via 0^0 + 699 cm^{-1}
via 0^0 + 700 cm^{-1}
28^2m^1
$26^128^1m^1$ m^2 m^4 m^5
17^1m^1 m^2 m^4 m^5
15^1m^1 m^1 m^4 m^5
m^2 m^4 m^5
30^1m^2
29^1m^2
via a_1 symmetry bands
via 0^0 + 701 cm^{-1}
via 0^0 + 702 cm^{-1}
via 0^0 + 704 cm^{-1}
via 0^0 + 706 cm^{-1}
$26^129^1m^0$
$19^130^2m^{3(+)}$
$18^229^1m^{3(-)}$
$18^129^1m^{3(-)}$
28^2m^0
$18^126^129^1m^0$
$20^121^1m^{3(+)}$
$17^1m^{3(+)}$
$26^128^1m^{3(+)}$
$m^{3(+)}$
$29^1m^{3(-)}/m^{6(-)}$
17^1m^0
$26^128^1m^0$
$15^1m^{3(+)}$
$m^{6(+)}$
$26^1m^{3(-)}$
$20^121^1m^{6(+)}$
0
200
400
600
800
1000
1200
Wavenumber relative to D_0^+ origin / cm^{-1}

Figure 8

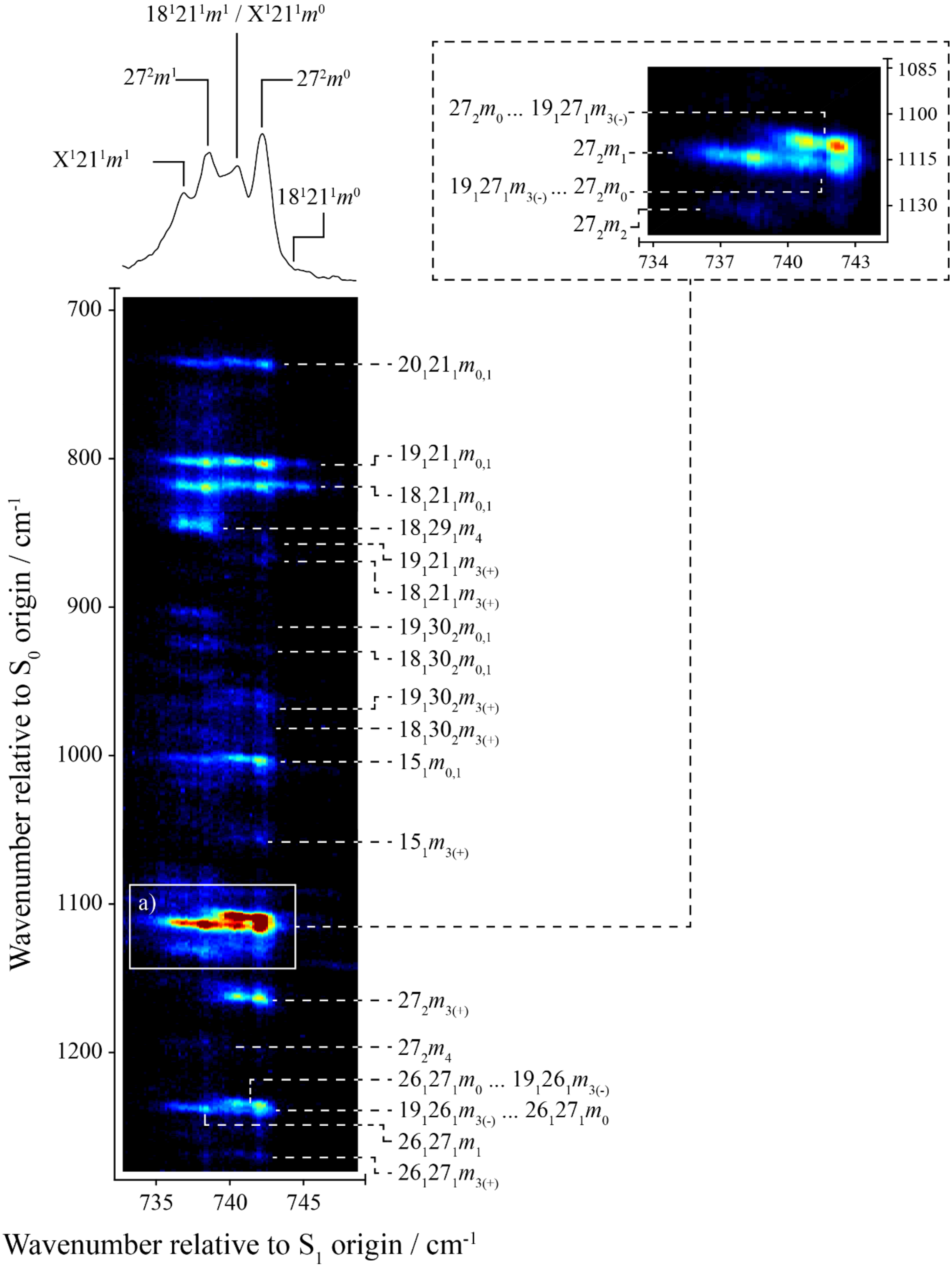
$18^1 21^1 m^1$ / $X^1 21^1 m^0$
$27^2 m^1$
$27^2 m^0$
$X^1 21^1 m^1$
$18^1 21^1 m^0$
$27_2 m_0$ … $19_1 27_1 m_{3(-)}$
$27_2 m_1$
$19_1 27_1 m_{3(-)}$ … $27_2 m_0$
$27_2 m_2$
1085
1100
1115
1130
734
737
740
743
700
800
900
1000
1100
1200
a)
$20_1 21_1 m_{0,1}$
$19_1 21_1 m_{0,1}$
$18_1 21_1 m_{0,1}$
$18_1 29_1 m_4$
$19_1 21_1 m_{3(+)}$
$18_1 21_1 m_{3(+)}$
$19_1 30_2 m_{0,1}$
$18_1 30_2 m_{0,1}$
$19_1 30_2 m_{3(+)}$
$18_1 30_2 m_{3(+)}$
$15_1 m_{0,1}$
$15_1 m_{3(+)}$
$27_2 m_{3(+)}$
$27_2 m_4$
$26_1 27_1 m_0$ … $19_1 26_1 m_{3(-)}$
$19_1 26_1 m_{3(-)}$ … $26_1 27_1 m_0$
$26_1 27_1 m_1$
$26_1 27_1 m_{3(+)}$
735
740
745
Wavenumber relative to S_0 origin / cm^{-1}
Wavenumber relative to S_1 origin / cm^{-1}

Figure 9

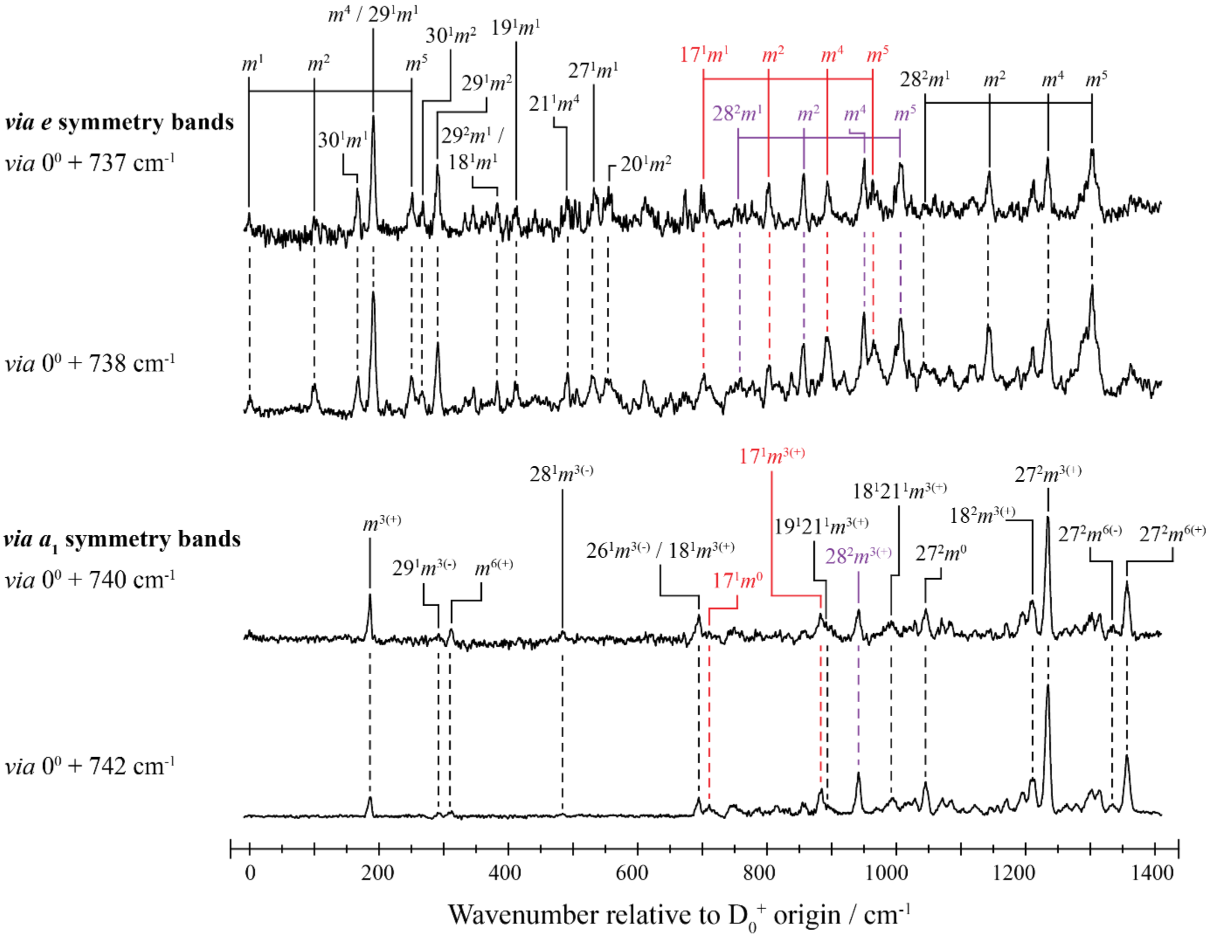

m^4 / 29^1m^1
30^1m^2
19^1m^1
m^1
m^2
m^5
29^1m^2
27^1m^1
17^1m^1
m^2
m^4
m^5
28^2m^1
m^2
m^4
m^5
21^1m^4
28^2m^1
m^2
m^4
m^5
via e symmetry bands
via 0^0 + 737 cm^{-1}
30^1m^1
29^2m^1 /
18^1m^1
20^1m^2
via 0^0 + 738 cm^{-1}
$17^1m^{3(+)}$
$28^1m^{3(-)}$
$27^2m^{3(+)}$
$18^121^1m^{3(+)}$
$18^2m^{3(+)}$
$19^121^1m^{3(+)}$
$m^{3(+)}$
via a_1 symmetry bands
$27^2m^{6(-)}$
$27^2m^{6(+)}$
$26^1m^{3(-)}$ / $18^1m^{3(+)}$
$28^2m^{3(+)}$
27^2m^0
$29^1m^{3(-)}$
$m^{6(+)}$
via 0^0 + 740 cm^{-1}
17^1m^0
via 0^0 + 742 cm^{-1}
0
200
400
600
800
1000
1200
1400
Wavenumber relative to D_0^+ origin / cm^{-1}

References

---

[1] D. J. Kemp, E. F. Fryer, A. R. Davies, and T. G. Wright J. Chem. Phys. **151**, 084311 (2019).

[2] A. R. Davies, D. J. Kemp, L. G. Warner, E. F. Fryer, A. Rees, and T. G. Wright J. Chem. Phys. **152** 214303 (2020).

[3] A. R. Davies, D. J. Kemp, and T. G. Wright AIP Adv. **10** 125206 (2020).

[4] L. D. Stewart, J. R. Gascooke, and W. D. Lawrance, J. Chem. Phys. **150**, 174303 (2019).

[5] K. Okuyama, N. Mikami, and M. Ito, J. Phys. Chem., **89**, 5617 (1985).

[6] P. A. Graham and S. H. Kable, J. Chem. Phys. **103**, 6426 (1995).

[7] V. L. Ayles, C. J. Hammond, D. E. Bergeron, O. J. Richards, and T. G. Wright, J. Chem. Phys. **126**, 244304 (2007).

[8] A. M. Gardner, W. D. Tuttle, L. E. Whalley, and T. G. Wright, Chem. Sci. **9**, 2270 (2018).

[9] N. J. Reilly, T. W. Schmidt, and S. H. Kable, J. Phys. Chem. A **110**, 12355 (2006).

[10] J. R. Gascooke and W. D. Lawrance, Eur. Phys. J. D **71**, 287 (2017).

[11] D. J. Kemp, W. D. Tuttle, F. M. S. Jones, A. M. Gardner, A. Andrejeva, J. C. A. Wakefield and T. G. Wright, J. Molec. Spectrosc. **346**, 46 (2018).

[12] A. M. Gardner, W. D. Tuttle, P. Groner, and T. G. Wright, J. Chem. Phys. **146**, 124308 (2017).

[13] E. Fermi, *Z. Phys*., 1931, **71**, 250.

[14] D. J. Nesbitt and R. W. Field, *J. Phys. Chem*., 1996, **100**, 12735.

[15] N. T. Whetton and W. D. Lawrance, J. Phys. Chem. **93**, 5377 (1989).

[16] J. R. Gascooke and W. D. Lawrance, J. Chem. Phys. **138**, 134302 (2013).

[17] A. M. Gardner, W. D. Tuttle, L. Whalley, A. Claydon, J. H. Carter and T. G. Wright, J. Chem. Phys. **145**, 124307 (2016).

[18] W. D. Tuttle, A. M. Gardner, L. E. Whalley, D. J. Kemp and T. G. Wright Phys. Chem. Chem. Phys. **21** 14133 (2019).

[19] D. J. Kemp, W. D. Tuttle, A. M. Gardner, L. E. Whalley and T. G. Wright J. Chem. Phys. **151**, 064308 (2019).

[20] W. D. Tuttle, A. M. Gardner, L. E. Whalley and T. G. Wright J. Chem. Phys. **146**, 244310 (2017).

[21] D. J. Kemp, A. M. Gardner, W. D. Tuttle and T G. Wright Molec. Phys. **117**, 3011 (2019).

[22] D. J. Kemp, L. E. Whalley, A. M. Gardner, W. D. Tuttle, L. G. Warner and T. G. Wright J. Chem. Phys. **150**, 064306 (2019).

[23] A. M. Gardner, L. E. Whalley, D. J. Kemp, W. D. Tuttle and T. G. Wright J. Chem. Phys. **151**, 154302 (2019).

[24] A. R. Davies, D. J. Kemp, and T. G. Wright, J. Chem. Phys. **15** 224305 (2021).

---

[25] D. J. Kemp, A. M. Gardner, W. D. Tuttle, J. Midgley, K. L. Reid and T. G. Wright J. Chem. Phys. **149** 094301 (2018).

[26] D. J. Kemp, L. G. Warner and T. G. Wright, J. Chem. Phys. **152**, 064303 (2020).